Effective refractive index and group velocity determination of 3D photonic crystals by means of white light interferometry

J. F. Galisteo-López[a,b], M. Galli[b], M. Patrini[b], A. Balestreri[b], L. C. Andreani[b] and C. López[a]*

[a)]*Instituto de Ciencia de Materiales de Madrid (CSIC) and Unidad Asociada CSIC-Universidad de Vigo, Cantoblanco 28049, Madrid, Spain*

[b)]*Dipartimento di Fisica "A. Volta", Università degli Studi di Pavia, Via Bassi 6, I-27100 Pavia, Italy*

White-light interferometry measurements over a wide spectral range in the optical region have been performed on three dimensional (3D) opal-based photonic crystals that have permitted extracting the optical phase delay introduced by samples with an increasing number of layers. The absolute phase that corresponds to the wavevector inside the samples has been obtained by a proper normalization procedure. From the absolute phase and the transmittance we have determined the complex effective refractive index of the 3D photonic crystals, whose real part shows normal dispersion outside the pseudogap and anomalous (negative) dispersion across the pseudogap. By a numerical derivative of the measured phase the group velocity is directly obtained, which displays slowing down at the band edge and superluminal behavior inside the photonic gap. The evolution of the measured quantities with sample thickness and their convergence towards the infinite crystal behavior are successfully compared to theoretical calculations of the optical properties for the finite system as well as of the energy bands. The role of structural disorder on the measured quantities is also discussed.

* Electronic mail: cefe@icmm.csic.es

1. Introduction

Photonic crystals[1-4] are artificial materials which permit modifying the propagation of electromagnetic radiation[5] and the decay dynamics[6] of excited light sources in ways not allowed by conventional materials. This is directly related to the peculiar dispersion relation for such structures, which takes place in the form of allowed and forbidden frequency intervals for light propagation, as a consequence of Bragg diffraction. The latter is caused by the spatial periodicity present in the dielectric function of the crystal, which scatters light coherently in a manner analogous to that of the crystal potential acting on electronic waves in conventional semiconductors. Among the different routes to fabricate three dimensional (3D) photonic crystals, self assembly stands out for ease of fabrication and low cost.[7]

Reflection and transmission spectroscopy are nowadays the most widespread techniques for the optical characterization of three dimensional photonic crystals. They are usually employed to detect the existence of forbidden spectral intervals, known as stop bands. These appear as regions of low (high) transmission (reflection), indicating the exponential attenuation of electromagnetic radiation as it propagates through the crystal. One major drawback of these techniques is that they usually fail to provide information on the dispersion of the photonic bands and knowledge is gained only on the existence of stop bands. Vlasov and co-workers[8] reported on spectroscopic reflection measurements on artificial opals with reduced refractive index contrast through which information was collected on the shape of energy bands. Such study was performed in the surroundings of the forbidden frequency interval appearing along the [111] direction in artificial opals and associated to first order Bragg diffraction by the {111} planes, commonly termed the L-pseudogap as it does not spread to other crystallographic directions. Such information was obtained from Fabry-Perot

oscillations originated from the interference between light reflected at the front and rear facets of the sample. This method is, however, limited by sample quality. As the thickness of the crystal increases, the contribution from the rear end of the crystal decreases as a consequence of light being scattered by defects and Fabry-Perot oscillations become less defined.

In order to explore the dispersive properties of 3D photonic crystals, phase sensitive techniques have been employed that have allowed the determination of the band structure in the surroundings of stop bands. Yablonovitch and Gmitter[9] extracted the band dispersion of a Yablonovite structure in the microwave regime for the main directions within the first Brillouin zone. Later on, Watson and co-workers[10,11] used a modified Mach-Zehnder interferometer (MZI) to measure the phase delay introduced by colloidal crystals in the vicinity of the L-pseudogap. For those frequencies contained within the L-pseudogap, the phase upon reflection was recently measured using artificial opals as reflectors of a Fabry-Perot cavity.[12] Another method for determining the band structure of a 3D crystal, not based on a phase sensitive technique, is that introduced in Ref. 13. In this approach, studying light refraction of monochromatic beams propagating through the system allowed obtaining equi-frequency surfaces from which the band structure was reconstructed.

The above mentioned techniques also fail to provide information on the dynamics of light propagating through the crystal. In this case time resolved experiments have proven to be a valuable tool. The main interest in 3D photonic crystals has been placed on the spectral region close to the pseudogap edges, where energy bands bend near the edge of the Brillouin zone. This band bending implies a reduction in group velocity which increases the interaction time of electromagnetic radiation with the crystal. Also in a narrow spectral range around the pseudogap, time resolved experiments were

performed using ultra-short pulses and a group velocity reduction was measured near the gap edges.[14,15] In the case of Ref. 15, the group velocity dispersion was also measured. Very recently, the group velocity and its dispersion were determined in a wide spectral region around the pseudogap by means of white light interferometry on artificial opals[16].

In this work phase sensitive measurements are presented on self-assembled, 3D photonic crystals consisting of artificial opals with an increasing number of layers and different lattice parameters. Employing white-light interferometry in the time domain the phase delay introduced by the samples is measured, which allows determining the dispersion relation over a large spectral range in the optical region. Care is taken in defining the absolute phase and in obtaining its frequency dependence with the correct normalization, *i.e.*, after subtracting the phase introduced by the substrate. From the absolute phase delay, the real part of the effective refractive index of the 3D photonic crystal is unambiguously determined for the first time, and is shown to present a region of anomalous dispersion across the pseudogap. From transmittance measurements the imaginary part of the effective refractive index is obtained which provides information on light extinction by the samples due to both Bragg scattering and disorder. Taking the first derivative of the measured phase we obtain the group velocity v_g/c (or the group index $n_g=c/v_g$) which exhibits pronounced slowing down at the band edge and superluminal behavior within the photonic gap. Its evolution with sample thickness and its convergence towards the behavior predicted for the infinite crystal by the calculated energy bands is discussed. A comparison between experimental results and theoretical calculations for the finite system shows an excellent agreement. Small deviations near the low energy edge of the pseudogap are observed and point to the effect of structural disorder.

2. Experimental

The samples used in the present work are artificial opals made of polystyrene spheres of two different diameters (*i.e.* 505 and 705 nm, 3% polydispersity, values obtained from transmission electron microscopy –TEM- measurements) and controlled thickness, grown on glass substrates. Details on fabrication and previous optical characterization by means of reflection and transmission spectroscopy can be found elsewhere.[17] The experimental set-up employed in the present work is that used in Ref. 18 and 19 for probing the dispersive properties of silica substrates and dielectric mirrors respectively. It consists of a modified Mach-Zehnder Interferometer (MZI) coupled to a commercial scanning Michelson interferometer (SMI). The sample is introduced in one of the arms of the MZI (sample arm) and the other one remains empty (reference arm). The signal collected by the detector in the SMI as a function of the distance traveled by its moving mirror yields an interferogram, from which the phase delay introduced by the sample is obtained by means of Fourier analysis. In order to remove the contribution to the phase delay introduced by the glass substrate, a reference measurement was performed in a region nearby the sample where only the glass substrate was exposed. Then, the phase delay introduced by the opal sample alone was obtained simply by subtraction of the two contributions. This procedure has the advantage to completely eliminate any spurious phase-shift coming from the instrumental apparatus, and for this reason it assures very precise values of the measured phase.[18] Furthermore, in order to assure the proper phase normalization, the thickness of the substrate was checked to be the same in both the sample and reference measurements. This was done by translating the substrate across the probe beam and observing the separation between the auto- and the cross-correlation lobes in the interferogram, which directly yields the optical path

difference between the different regions of the substrate. By assuming a refractive index value of 1.51 for the glass substrate as provided by the manufacturers (Menzel-Glaser), the substrate thickness was observed to vary by no more than 100 nm over distances of 2 mm. This thickness variation, albeit small, has to be considered as a possible source of error in the measurements. Therefore, the sample areas to be probed (~125 μm) were chosen so that an exposed substrate region was available as close as possible (typically ~300 μm), leading to an upper bound to the error in the measured phase of about 0.18 radians, which can be assumed as the experimental error in the phase determination.

3. Theoretical model

In order to model the optical response of the opal photonic crystals we calculate the transmittance $T(\omega)$ and the phase delay $\phi(\omega)$ of the light beam transmitted through the sample by means of the scattering-matrix method,[20] which is a fully vectorial treatment of Maxwell equations in 3D. The dispersion of the refractive index of polystyrene is taken into account by using published data.[21] For this reason we adopt absolute energy units rather than the widely used adimensional reduced frequency a/λ. Notice that each period of the fcc structure viewed along [111] (which coincides with the propagation direction at normal incidence) consists of three layers containing spheres arranged in a triangular lattice, where each layer is shifted with respect to the previous one in a direction perpendicular to [111]. Since the scattering-matrix method requires the crystal being divided into homogeneous layers along the propagation direction, we subdivide each dielectric sphere into cylinders with their axis oriented along the [111] direction and with the same total volume as that of the spheres. Such an approach is found to yield good results in terms of reproducing the band structure of the infinite system of spheres as well as the experimental results for the finite system, as it

will be shown below. The diameters and heights[22,23] of the cylinders are optimized in order to reproduce the photonic bands of the opal structure with spheres. In Fig.1 we show a comparison of the calculated photonic bands for the fcc structure with dielectric spheres and cylinders, respectively. Along the main directions of the Brillouin zone (*i.e.*, for propagation along [111]) the bands are in very good agreement even for energies higher than the spectral range probed in the present experiments. In order to reproduce the experimental results, including out-of-plane diffraction measurements, we had to assume an average sphere diameter of 708 nm and a lattice constant of 725-730 nm in the planes perpendicular to the [111] direction, slightly larger than the values determined from TEM measurements but still within the 3% polydispersity. The calculations assuming these parameters are found to be in very good agreement with the experimental results, as discussed in the next Sections.

4. Phase delay and effective refractive index

When the reference arm in the MZI is blocked, the transmittance T(ω) from the sample can be obtained. In this way we measure both the phase delay and the transmittance at the same point of the sample. This is done for samples of increasing thickness and different lattice parameter. Fig. 2 represents transmittance measurements for samples made of nominally 705 nm spheres and having an increasing number of layers. A pronounced dip in transmittance can be appreciated taking place for an energy of 0.76 eV, associated to the stop band (L-pseudogap) opening in the dispersion relation as a consequence of Bragg diffraction by the {111} planes parallel to the sample surface. As the number of layers increases, such dip becomes more pronounced as expected due to a more efficient Bragg diffraction. Also evident in the spectra is a region of low transmittance outside of the stop band which decreases towards high

frequencies. In this spectral region secondary oscillations are present which are associated with the finiteness of the sample and which allows determining its thickness.[17] Moreover, the transmittance outside the stop band decreases with sample thickness, a behavior known to be associated with extinction by structural disorder.[24,25] The role of disorder in the present measurements will be further discussed below.

Figure 3 shows the phase delay and the transmittance for a sample 18 layers thick. Here it is evident that in the same spectral region where the dip was observed in the transmittance spectra a jump in the measured phase is present. Such jump will be discussed in detail below. As for transmittance, the phase delay has been measured for samples having an increasing number of layers.

Since the phase delay is obtained by Fourier analysis, it carries an uncertainty of $m \cdot 2\pi$, where m is an integer number. The absolute phase $\phi(\omega)$ is a continuous function which vanishes linearly in frequency for $\omega \rightarrow 0$.[26] In order to determine the absolute phase an integer multiple of 2π must be added/subtracted from the measured one. To obtain the number m one may, as a first approximation, linearly extrapolate the phase to the low-energy region and force it to vanish for zero frequency. This approach yields a value of m, which may be corrected, if necessary, by considering the effective refractive index, as explained at the end of this Section. By doing this we have obtained the phase delay introduced by our samples in a wide spectral range between 0.5 and 1.3 eV, corresponding to the L-pseudogap and its surroundings. Figure 4a shows the evolution of the phase delay as the number of layers is increased. For a small number of layers it is just a straight line, resembling the behavior of a transparent homogeneous material. As the thickness of the crystal increases, the slope of the phase as a function of frequency increases as expected for an increasing optical path. Further, a slower change of the phase occurs for those frequencies within the L-pseudogap, indicated by dashed

horizontal lines in the figure. A similar jump is known to take place across the forbidden intervals of 1D photonic crystals[19] and to be a signature of Bragg diffraction. In the present 3D case we would expect a similar behavior for this particular orientation and energy range for which Bragg diffraction occurs. At variance with previous determinations of phase delay for similar systems,[10,11] here the thickness of the samples is such that enough signal is collected for frequencies within the pseudogap. Theoretical calculations are also plotted in Fig. 4 for comparison. The overall agreement between theory and experiment is satisfactory. Calculations reproduce the overall shape and absolute value of the phase delay on the spectral range considered. A slight deviation is observed in the low energy side of the phase jump, which increases with sample thickness. This can be better appreciated in Fig. 4b, where results for the thickest measured sample are blown up. This disagreement, which points to the effect of structural disorder, will be discussed in a following section. We notice that the theoretical value for the phase delay is an absolute one, as the calculated phase starts from $\omega=0$ and is rendered continuous (or "unwrapped") by adding appropriate multiples of 2π. The agreement between experiment and theory also validates the experimental determination of the absolute phase.

Once the phase delay and the transmittance of the samples are known, the real and imaginary parts of the effective refractive index n_{eff} can be obtained. The definition of effective refractive index used here is that introduced in reference 27 for 1D photonic crystals, which has been proven to satisfy Kramers-Kronig relations and to correctly describe the dispersive properties of such structures, especially in terms of the possibility of fulfilling phase matching conditions for second harmonic generation. This n_{eff} has also been used to successfully account for the observation of third harmonic generation in 3D samples similar to the ones used in the present

measurements,[28] and second harmonic generation in dye doped colloidal crystals.[29] This definition of n_{eff} accounts for the dispersive properties of a *finite* sample along the direction of propagation, in the sense that a homogeneous medium described by n_{eff} has exactly the same transmittance and phase delay as the real sample. At this point, and for the sake of clarity, it must be noticed that such definition is different from that introduced in reference 5. The latter refers to an effective refractive index defined for the *infinite* crystal from equifrequency surfaces (EFS), that is, the set of all allowed wave vectors for a given frequency. In the spectral regions where the band structure is so that spherical EFS may be found, the effective refractive index accounts for the refractive properties of the crystal. Such regions are to be found in the low frequency limit as well as close to frequency gaps.[5,30]

To specify the present definition of the effective refractive index, following Reference 27, we write the complex transmission function of the sample as $t(\omega) = |t|e^{i\phi}$ (where t is the square root of the transmittance T(ω)) and define the complex refractive index as follows:

$$n_{eff} = \mathrm{Re}(n_{eff}) + i\,\mathrm{Im}(n_{eff}) = \frac{c}{\omega D}\left(\phi(\omega) - i\log|t|\right) \quad . \qquad (1)$$

The sample thickness is $D = d_{111}N$, where $d_{111} = a/(3)^{1/2}$ is the interplanar distance for the (111) planes parallel to the surface and N the number of such planes. In the following we discuss the behavior of the real and imaginary parts separately.

Therefore, from the phase delay we can extract the real part of the effective refractive index $\mathrm{Re}(n_{eff})$ for our crystals without any additional assumption. In this way we have extracted $\mathrm{Re}(n_{\text{eff}})$ for samples with an increasing number of layers. The results are plotted in Fig. 5a. The effective refractive index has an overall increase with frequency, except for energies around ~0.76 eV corresponding to the pseudo-gap,

where a region of anomalous dispersion (i.e., decreasing refractive index with increasing frequency) occurs. This region becomes more evident as the thickness of the sample is increased. In homogeneous materials anomalous dispersion is associated with spectral regions where absorption or gain takes place. In the present situation the origin of this phenomenon is related to extinction by Bragg diffraction, as in the 1D case.[27] In order to validate this statement, the scalability of the experimental results was checked by measuring samples with 505 nm spheres. The region of anomalous dispersion shifts to higher frequencies (1.05 eV) showing scalability with lattice parameter and therefore may be associated with Bragg diffraction due to the periodicity of the structure and not to absorption of the materials comprising the crystal. In addition, in the 705 nm sphere samples regions of anomalous dispersion due to water vapor absorption are seen at both sides of the main feature discussed. As the crystal thickness increases the former region, corresponding to the pseudo-gap, becomes spectrally narrower. This evolution coincides with that of the reflectance peak[17] as expected, both features being associated with extinction due to Bragg diffraction. Also the spread of $Re(n_{eff})$ across the pseudo-gap increases as a function of crystal thickness. This corresponds to the fact that Bragg diffraction (and therefore extinction) becomes more efficient with increasing number of planes. This shows that if second or third harmonic generation is to be observed in such systems, as in Refs. 28 and 29, the size of the crystal will be crucial in achieving the phase matching condition. Theoretical results also reproduce the above mentioned trend. A small difference between experiment and theory is evident at the low and high energy regions of normal dispersion. Such a deviation is rather small and, at the lowest energy of 0.5 eV, it decreases with the sample thickness from 1% for the 10 layer sample to 0.3% for the 40 layer one. The decrease of the deviation with sample thickness could be associated with the fact that thinner samples present a slightly lower filling fraction as

compared to the thicker samples, so that an effective medium approach is more realistic for the latter. Such structural variations are currently under study. Here we must also point out a divergence between the values obtained for $Re(n_{eff})$ by theory and experiment at the low energy edge of the anomalous dispersion interval (L-pseudogap). Such discrepancy is expected as being related to the deviation already observed in the phase delay results (see Fig. 4).

These results represent a clear improvement with respect to previous phase delay data measured in colloidal crystals.[10,11] On one hand, the good quality and reduced thickness of the samples allow measuring the phase delay for frequencies within the pseudogap, not observed previously due to the weak signal in thicker crystals. The present data then represent the first full determination of the effective refractive index according to Ref. 27, showing anomalous dispersion across the entire pseudogap, of a 3D photonic crystal in the optical region. Further, the increased refractive index contrast of our samples with respect to the above mentioned colloidal crystals allows observing a variation in $Re(n_{eff})$ of up to 0.04 across the pseudogap edges. This value is an order magnitude larger than that obtained with colloidal crystals having 1000 planes.

At this point we would like to explain in more detail the procedure used for determining the absolute phase. Since the spectral range accessible to the measurements is $\hbar\omega>0.5$ eV, extrapolating the measured phase to zero frequency carries an uncertainty due to the dispersion of the sample refractive index. This uncertainty is negligibly small (i.e., much smaller than 2π) for thin samples, while for thick samples it may prevent from retrieving the absolute phase by linear extrapolation to $\omega\rightarrow 0$. In order to obtain the absolute phase, the value of m determined by low-frequency extrapolation may be corrected self-consistently as follows. By adding/subtracting $m\cdot 2\pi$ to the measured phase and calculating the effective refractive index $Re(n_{eff})$ of the samples, one realizes

that it exists only one value of the integer number *m* that gives a physically correct value for $Re(n_{eff})$ and for its dispersion. This can be appreciated in Fig. 6, where the real part of the effective index calculated from the phase delay introduced by a 20 layer thick sample is shown after subtracting different multiples of 2π (close to m=9 estimated by linear extrapolation to $\omega \rightarrow 0$). If *m* is chosen too large (m=10 in Fig. 6), $Re(n_{eff})$ presents anomalous dispersion across the whole spectral range considered, and a value much higher than that predicted by effective-medium theory. On the contrary, if *m* is chosen too small (m=8 in Fig. 6), the obtained values for $Re(n_{eff})$ show too large dispersion and are below those predicted by theory by more than 15%. This self-consistent procedure was carried through for all samples and it confirms that the phase results presented in Figs. 3a and 4 refer indeed to the absolute phase, in agreement with the theory.

We have extracted $\mathrm{Im}(n_{eff})$ from Eq. (1) for the same samples for which its real counterpart was presented in Fig. 5a, and the results are shown in Fig. 5b. Theoretical predictions are plotted together with the experiment. They reproduce well the overall spectral behavior of $\mathrm{Im}(n_{eff})$ with a flat background for frequencies outside the pseudogap and a pronounced peak for frequencies within the pseudogap, which accounts for light extinction due to Bragg diffraction. Nevertheless, an additional physical effect is evident when comparing theory and experiment; extinction outside the stop band is larger in the experiment for frequencies outside the pseudogap. Such behavior is known to be due to extinction of light caused by scattering by structural disorder.[24,25]

Finally it is interesting to compare the evolution of $\mathrm{Im}(n_{eff})$ with the number of layers both for a frequency inside the stop band and for a frequency outside it. Such comparison is presented in Fig. 7. It is evident that two opposite trends are present in

the figure. On the one hand, extinction for frequencies contained inside the gap increases with the number of layers (Fig. 7a) and seems to reach a stationary behavior for samples with N~30 layers. This is to be expected since as the number of layers increases, extinction due to Bragg diffraction becomes more effective and hence the imaginary component of the refractive index increases towards the infinite crystal limit. On the other hand if we consider a frequency outside from the stop band (Fig. 7b) we can see that extinction becomes less effective with increasing sample thickness. The latter result indicates that the amount of disorder, which is the only mechanism for extinction in this spectral range where Bragg diffraction does not occur and polystyrene does not absorb, is smaller for thicker samples. This finding is supported by previous evidence from scanning electron micrographs as well as from the broadening of optical diffraction patterns from similar samples.[31, 32] Thus we may conclude that the analysis of the imaginary part of the effective refractive index yields useful information on Bragg diffraction within the pseudogap as well as on the effects of structural disorder.

5. Group velocity

Once the phase delay is measured, the effective dispersion relation of the sample can be obtained in a straightforward manner as $k(\omega)=\phi(\omega)/D$. Then one may obtain the group velocity v_g associated with propagation along the ΓL direction which is just the derivative of the dispersion relation with respect to the frequency. In our case it is the inverse group velocity normalized to the speed of light in vacuum that we calculate. Such quantity is commonly termed group index n_g:[27]

$$n_g = \frac{c}{v_g} = \frac{c}{D}\frac{d\phi}{d\omega} \qquad (2)$$

The group velocity can be defined as the velocity at which the peak amplitude of a light pulse traverses a medium. Therefore it provides information on the dynamics of light propagation through that medium. For an infinite photonic crystal, v_g at a certain frequency may be calculated as the slope of the corresponding band at that frequency. In the case of no extinction, v_g equals the energy velocity, that is the speed at which electromagnetic energy propagates.[30] In the absence of available electromagnetic states neither of them is defined as no energy can propagate through the medium. But for a finite photonic crystal the situation is different. Here, for frequencies located within a forbidden interval, light will be exponentially attenuated but it may still be transmitted through the crystal. In the presence of extinction, v_g does not equal the energy velocity[33] and care must be taken when interpreting experimental results.

In Fig. 8 the evolution of n_g extracted from Eq. (2) is plotted for samples having an increasing number of layers. Some interesting points must be noted in this graph. For samples just 10 layers thick n_g has small variations with frequency. Noisy regions appear which correspond to the anomalous dispersion associated with water vapor absorption also observed in the results for n_{eff}. As the thickness increases, two peaks of n_g develop at frequencies close to the pseudogap edges (indicated by dotted vertical lines), and a region of low n_g appears in between. For an increasing number of layers the two peaks become more pronounced and shift closer to the position of the pseudogap edges. Far from these frequencies n_g presents oscillations around a constant value. Such oscillations coincide with Fabry-Perot resonances observed in reflectance and transmittance,[16,19] and are a result of the finite size of the sample.

Near the edges of the pseudogap, energy bands separate from the low energy linear behaviour and become flat. Thus, the v_g associated with the frequencies near the edges becomes extremely low. For an ideal infinite crystal the modes with these frequencies

become standing waves. For real finite crystals these "heavy" photons with such frequencies experience a very long optical path inside the structure, and their interaction time with the crystal is enhanced.[34] By introducing non linear optical materials in 1D photonic crystals this effect may lead to optical limiting and switching,[35] and to enhanced second harmonic generation by adequately tailoring the dispersion relation of the crystal.[27] If active media are introduced instead, enhanced emission[36] and gain could be achieved.[34,37] In the results presented in Fig. 8 the two peaks of n_g correspond to the spectral interval where anomalous dispersion was observed and may then be identified with the appearance of Bragg diffraction by the {111} planes parallel to the sample surface. This evolution can then be considered as a signature of the formation of the energy bands in this spectral region, where the decrease in v_g (and hence an increase in n_g) can be associated with the bending of the energy bands near the pseudogap. The observed increase in n_g reaches a maximum of n_g =2.5 at the high energy edge of the pseudogap. This is larger than previous n_g enhancements observed in colloidal crystals with ~1400 planes,[15] and in thin film opals with fewer layers.[16] As in the variations regarding the effective refractive index, increasing the photonic strength of our system by augmenting the refractive index contrast allows the observation of phenomena related to band edge bending in thinner samples, which show a sufficiently large signal within the pseudogap.

For frequencies within the pseudogap, the group index is observed to take on values below those in the long wavelength limit and even smaller than unity for samples only 15 layers thick. Such values of the group index correspond to superluminal values of the group velocity (*i.e.* v_g >c). This is in agreement with the approximate formula $v_g/c=Nd_{111}\Delta\omega_g/(\pi c)$, which follows from the phase variation of π across the photonic gap.[19] Superluminal group velocities have been experimentally observed with pulses

propagating through 1D photonic crystals[38,39] and also extracted from phase delay measurements.[16,19] Such results, although striking, are known not to be at odds with causality. For a finite system the group and energy velocities are not the same in those spectral regions where strong extinction takes place *(i.e.* inside the pseudogap), and the energy velocity remains below *c* for all frequencies.[33]

The measured group indices are well reproduced by theoretical calculations, as can be seen in Fig. 8. Not only the spectral position of the main features near the pseudogap edges, but also the modulations in n_g associated with Fabry-Perot oscillations far from the edges are in good agreement. The main discrepancy comes, as in the case of the phase and effective index, with the low energy edge of the pseudogap. Here theory predicts a value for n_g larger than the measured one. This is due to the fact that slowing at frequencies close to the pseudogap edges is not only related to gain or SHG enhancement. The fact that photons experience a longer optical path for these frequencies implies that they are more likely to be scattered by defects in the lattice. This was already observed in Ref. 17 for similar samples as an enhancement of the diffuse intensity generated inside the crystal. One may compare the frequency dependence of the optical response in reflectance, transmittance and diffuse intensity (1-R-T) of a 42 layer thick sample -extracted from Ref. 17- with the group index, as in Fig. 9. In the low energy edge there is a clear enhancement of diffuse intensity which coincides with a smaller group index, as compared to the high energy edge (where no enhancement of diffuse intensity is present). Such an asymmetry in the values for n_g is not present in the theoretical calculations, on the contrary a smaller inverse asymmetry should be observed. It seems that the generation of diffuse intensity counteracts the effect of sample thickness in the evolution of the n_g, which is expected to increase with the number of layers near the pseudogap edges. This fact has been also discussed in Ref.

16, and reproduced with a heuristic model where extinction due to disorder was accounted for by introducing absorption in a 1D model. The effect of disorder in the present phase sensitive measurements is an interesting aspect that will be dealt with in the future.

6. CONCLUSIONS

In summary, we have presented a detailed study of the evolution of the phase delay and group velocity of light transmitted through opal-based 3D photonic crystals as a function of sample thickness. The real and imaginary parts of the complex effective refractive index have been extracted from the measured absolute phase (after the contribution from the substrate was taken into account) and transmittance, respectively. The real part of the effective refractive index shows an overall increase with frequency but it presents a region of anomalous dispersion across the pseudogap: knowledge of the whole dispersive behavior can be used to design nonlinear optical experiments on these systems. The imaginary part provides information on Bragg diffraction as well as on scattering by structural disorder in the finite system. Finally, from the derivative of the measured phase, the group velocity has been extracted as a function of the number of layers. The evolution of all these physical quantities towards the infinite crystal behavior has been discussed and agrees with predictions from calculated energy bands. Experimental results for the optical response of the finite system are well reproduced by theoretical calculations in a fully vectorial formulation. Small discrepancies taking place near the low energy edge of the pseudogap are believed to be originated by the effect of scattering by structural defects. White light interferometry is proven to be a valuable tool to explore the dispersive properties of 3D photonic crystals and the present results encourage us to carry out further characterization along crystal directions other than the

one perpendicular to the sample surface as well as to further explore the role of structural disorder.

Acknowledgements:

This work was partially financed by COST-P11 project from the European Science Foundation, PHOREMOST project IST-511616 from the European Community, MAT2003-01237 project from the Spanish Ministry of Science, and Spain-Italy Integrated Action HI2004-0367.

REFERENCES

[1] E. Yablonovitch, Phys. Rev. Lett. **58**, 2059 (1987).

[2] S. John, Phys. Rev. Lett. **58,** 2486 (1987).

[3] K. Sakoda, *Optical Properties of Photonic Crystals* (Springer-Verlag, Berlin, 2001).

[4] K. Inoue and K. Ohtaka, *Photonic Crystals: Physics, Fabrication and Applications* (Springer-Verlag, New York, 2004).

[5] M. Notomi, Phys. Rev. B **62**, 10696 (2000).

[6] P. Lodahl, A. F. van Driel, I. S. Nikolaev, A. Irman, K. Overgaag, D. L. Vanmaekelbergh, and W. L. Vos, Nature **430**, 654 (2004).

[7] C. López, Adv. Mater. **15**, 1679 (2003).

[8] Y. A. Vlasov, M. Deutsch, and D. J. Norris, Appl. Phys. Lett. **76**, 1627 (2000).

[9] E. Yablonovitch and T. J. Gmitter, Phys. Rev. Lett. **63**, 1950 (1989).

[10] I. I. Tarhan, M. P. Zinkin, and G. H. Watson, Opt. Lett. **20**, 1571 (1995).

[11] B. T. Rosner, G. J. Schneider, and G. H. Watson, J. Opt. Soc. Am. B **15**, 2654 (1998).

[12] E. Istrate and E. H. Sargent, Appl. Phys. Lett. **86**, 151112 (2005).

[13] M. Notomi, T. Tamamura, Y. Ohtera, O. Hanaizumi, and S. Kawakami, Phys. Rev. B **61**, 7165 (2000).

[14] Y. A. Vlasov, S. Petit, G. Klein, B. Honerlage, and C. Hirlimann, Phys. Rev. E **60**, 1030 (1999).

[15] A. Imhof, W. L. Vos, R. Sprik and A. Lagendijk, Phys. Rev. Lett. **83**, 2942 (1999).

[16] G. von Freymann, S. John, S. Wong, V. Kitaev, and G. A. Ozin, App. Phys. Lett. **86**, art. no.- 053108 (2005).

[17] J. F. Galisteo-Lopez, E. Palacios-Lidon, E. Castillo-Martinez, and C. Lopez, Phys. Rev. B **68**, art. no.- 115109 (2003).

[18] M. Galli, F. Marabelli, and G. Guizzetti, Appl. Opt. **42**, 3910 (2003).

[19] M. Galli, D. Bajoni, F. Marabelli, L. C. Andreani, L. Pavesi, and G. Pucker, Phys. Rev. B **69**, art. no.- 115107 (2004).

[20] D. M. Whittaker and I.S. Culshaw, Phys. Rev. B. **60**, 2610 (1999).

[21] N. G. Sultanova, I. D. Nikolov, and C. D. Ivanov, Opt. Quant. Electron **35**, 21 (2003).

[22] Each sphere is subdivided into five cylinders with radii $r_1 = r_5 = 0.2a$, $r_2 = r_4 = 0.308a$, $r_3 = 0.3535a$ and heights $h_1 = h_5 = 0.129a$, $h_2 = h_4 = 0.122a$, $h_3 = 0.204a$, respectively.

[23] Notice that the last (no.5) cylinders of a given layer lie in the same plane as the first (no.1) cylinders of the next layer, thereby mimicking the interpenetration between two consecutive layers of spheres.

[24] Y. A. Vlasov, M. A. Kaliteevski, and V. V. Nikolaev, Phys. Rev. B **60**, 1555 (1999).

[25] Y. A. Vlasov, V. N. Astratov, A. V. Baryshev, A. A. Kaplyanskii, O. Z. Karimov, and M. F. Limonov, Phys. Rev. E **61**, 5784 (2000).

[26] Due to Kramers-Kronig relations between $\ln(|t|)$ and ϕ, the phase $\phi(\omega)$ is an odd function of frequency.

[27] M. Centini, C. Sibilia, M. Scalora, G. D'Aguanno, M. Bertolotti, M. J. Bloemer, C. M. Bowden, and I. Nefedov, Phys. Rev. E **60**, 4891 (1999).

[28] P. P. Markowicz, H. Tiryaki, H. Pudavar, P. N. Prasad, N. N.Lepeshkin, and R. W. Boyd, Phys. Rev. Lett **92, art. no.** -083903 (2004).

[29] J. Martorell, R. Vilaseca, and R. Corbalan, Appl. Phys. Lett. **70**, 702 (1997).

[30] A. Yariv and P. Yeh, J. Opt. Soc. Am. **67**, 438 (1977).

[31] J. F. Galisteo-López, "An optical study of opal based photonic crystals", PhD Thesis, Universidad Autónoma de Madrid (2005).

[32] J. F. Galisteo-López and C. López, Proceedings of SPIE vol. **540**, p1 (2004).

[33] G. D'Aguanno, M. Centini, M. Scalora, C. Sibilia, M. J. Bloemer, C. M. Bowden, J. W. Haus, and M. Bertolotti, Phys. Rev. E **6303**, art. no.-036610 (2001).

[34] J. P. Dowling, M. Scalora, M. J. Bloemer and C. M. Bowden, J. Appl. Phys. **75**, 1896 (1994).

[35] M. Scalora, J. P. Dowling, C. M. Bowden and M. J. Bloemer, Phys. Rev. Lett. **73**, 1368 (1994).

[36] I. Bulu, H. Caglayan and E. Ozbay, Phys. Rev. B **67**, 205103 (2003).

[37] Y. A. Vlasov, K. Luterova, I. Pelant, B. Honerlage, and V. N. Astratov, Appl. Phys. Lett. **71**, 1616 (1997).

[38] A. M. Steinberg, P. G. Kwiat, and R. Y. Chiao, Phys. Rev. Lett. **71**, 708 (1993).

[39] C. Spielmann, R. Szipocs, A. Stingl, and F. Krausz, Phys. Rev. Lett. **73**, 2308 (1994).

FIGURE CAPTIONS

FIGURE 1 (color online): Red circles: photonic bands of a polystyrene opal consisting of close-packed spheres of diameter b=708 nm and dielectric constant ε=2.455 in air. Blue lines: photonic bands of the same fcc structure when each dielectric spheres is replaced by five cylinders oriented along the [111] direction.[22] Inset: Brillouin zone of the fcc lattice.

FIGURE 2: Transmittance spectra in a logarithmic scale for samples made from spheres of 705 nm nominal diameter, having different thickness. Top to bottom: 10, 15, 20, 28, 31, 35 and 40 layers.

FIGURE 3: (a) Phase delay introduced by a sample 18 layers thick made of spheres of diameter 705 nm. (b) Transmittance collected from the same spot on the sample as the phase delay.

FIGURE 4 (color online): (a) Absolute phase delay for samples having an increasing number of layers. Left to right: 10, 15, 20, 28, 31, 35 and 40 layers. (b) Detail of the results for the sample 40 layers thick in the vicinity of the pseudogap. Experimental data appear as red lines and theoretical calculations as black ones. Horizontal dashed lines indicate the edges of the L-pseudogap as extracted from band calculations.

FIGURE 5 (color online): Real (a) and imaginary (b) parts of the effective refractive index estimated from the absolute phase and transmittance, respectively, for different sample thicknesses: top to bottom 40, 31, 20 and 10 layers. Vertical dashed lines

indicate the edges of the L-pseudogap as extracted from band calculations. All samples are made of spheres with 705 nm nominal diameter. Experimental data appear as red lines and theoretical calculations as black ones.

FIGURE 6: Effective refractive index estimated for a 20 layers thick sample after subtracting three consecutive multiples of 2π from the measured phase (see text). The data in the middle correspond to the multiple obtained by linearly extrapolating the phase delay in the low energy region. The top/bottom curve corresponds to a multiple larger/smaller by one.

FIGURE 7: Evolution of the imaginary part of the effective refractive index as a function of the number of layers for a frequency contained within the gap (a) and outside of it (b).

FIGURE 8 (color online): Group index (n_g) for samples with increasing number of layers. Top to bottom: 40, 31, 20 and 10 layers. Horizontal dashed lines indicate the limit of superluminal velocity v_g=c. Vertical dotted lines indicate the pseudogap edges predicted by calculated bands. Experimental data appear as red lines and theoretical calculations as black ones.

FIGURE 9: (a) Band structure for a polystyrene opal along the ΓL direction. (b) Reflectance, (c) transmittance and (d) diffuse intensity for a 42 layers thick sample. (e) Group index for a 40 layers thick sample.

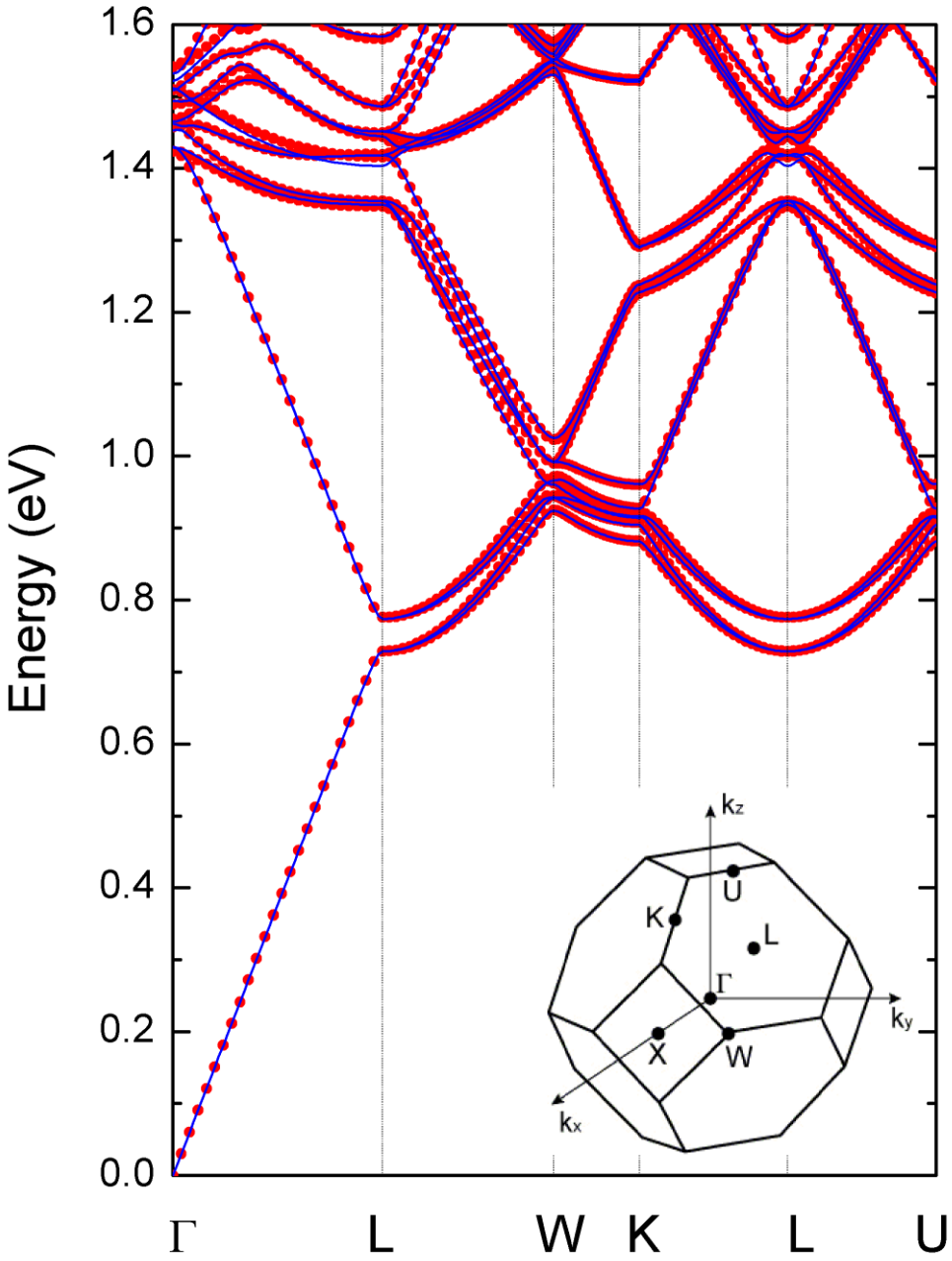

J.F. Galisteo-López *et al.* Figure 1

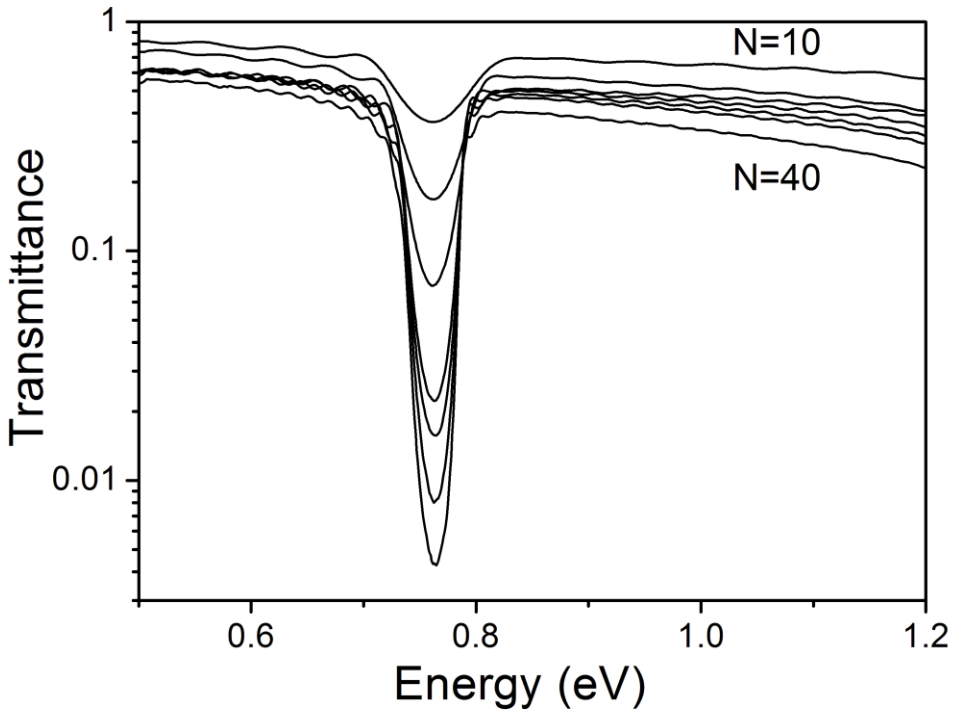

J.F. Galisteo-López *et al.* Figure 2

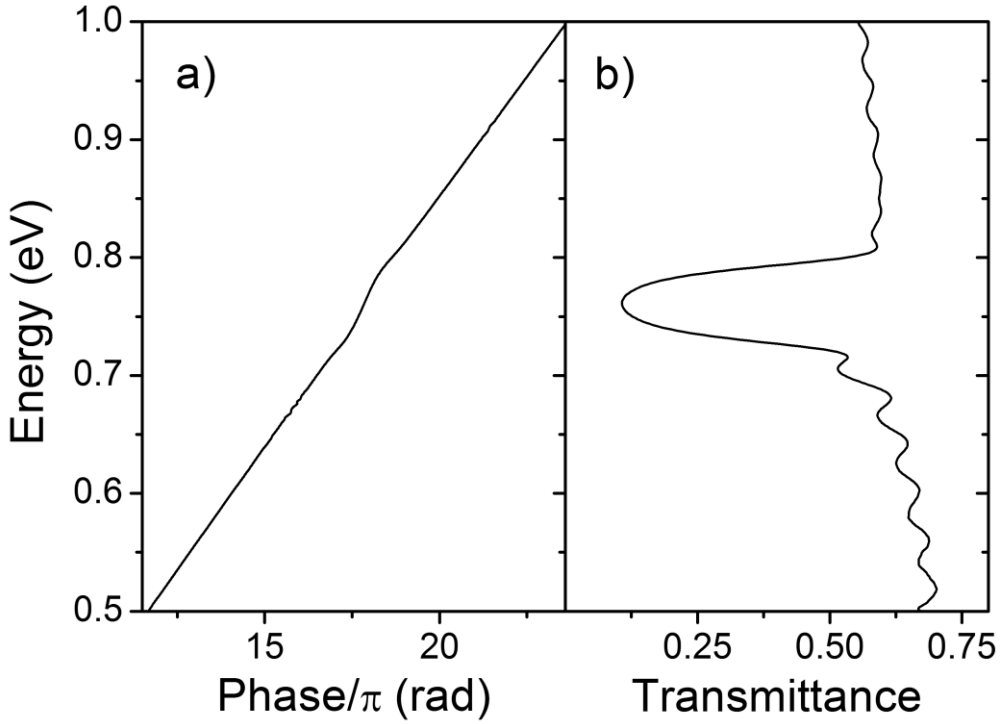

J.F. Galisteo-López *et al.* Figure 3

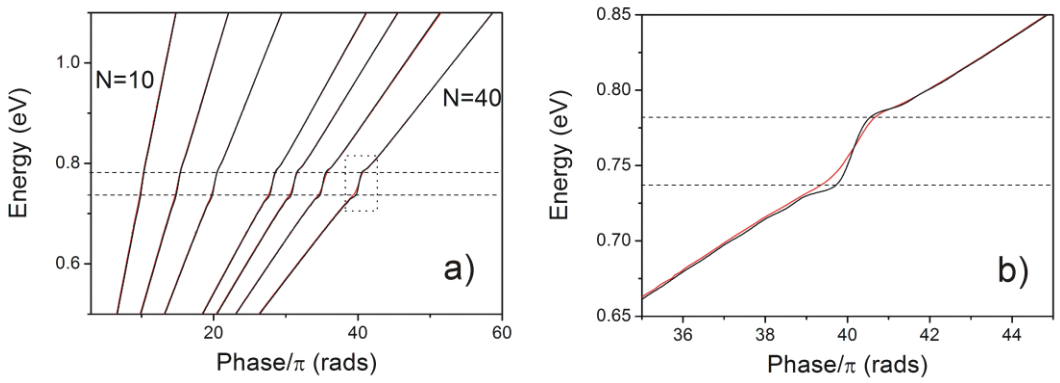

J.F. Galisteo-López *et al.* Figure 4

(Two column format)

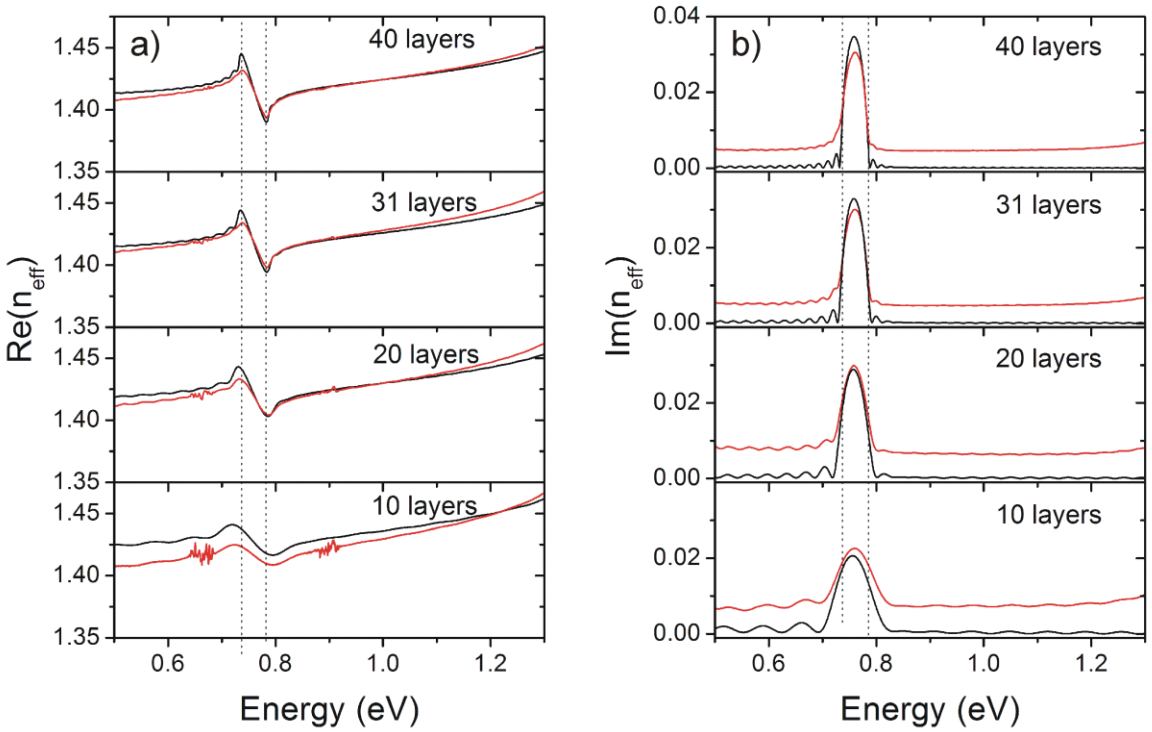

J.F. Galisteo-López *et al.* Figure 5

(Two column format)

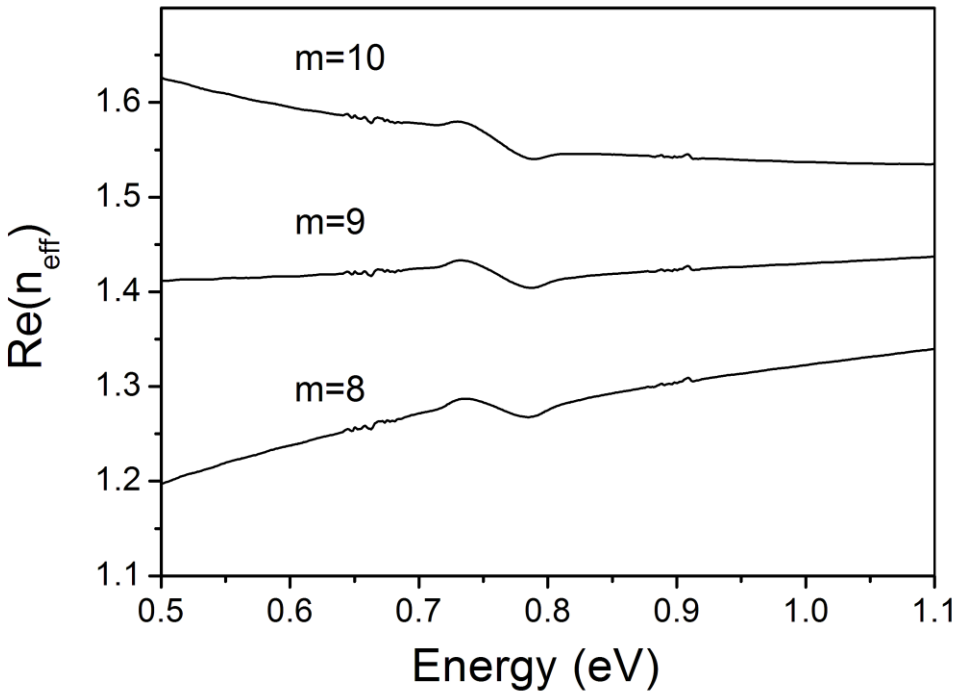

J.F. Galisteo-López *et al.* Figure 6

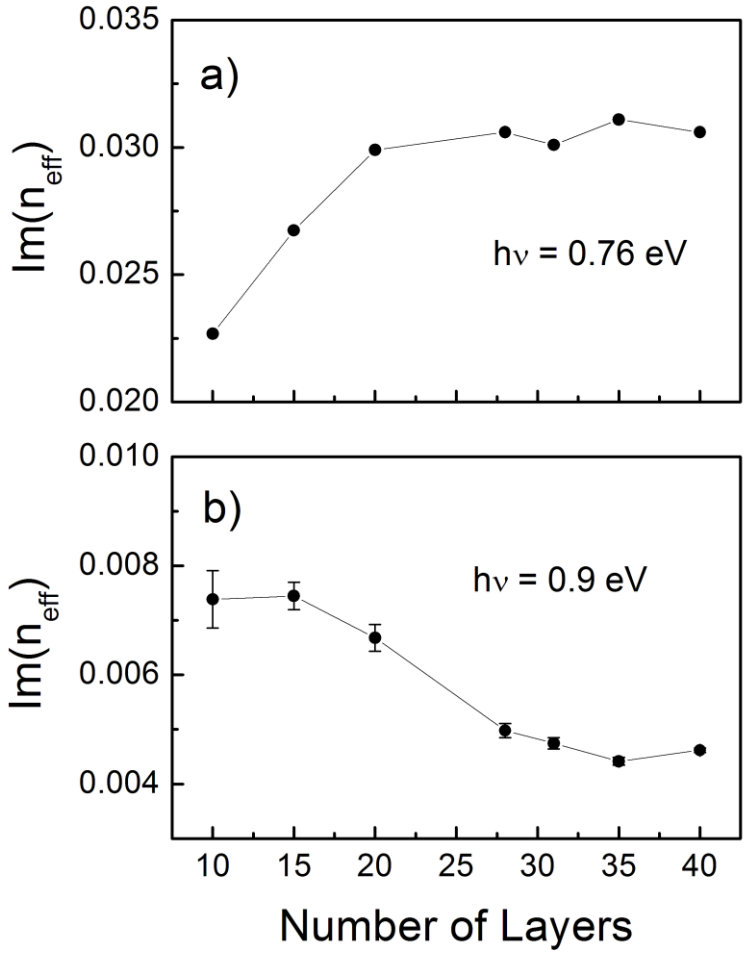

J.F. Galisteo-López *et al.* Figure 7

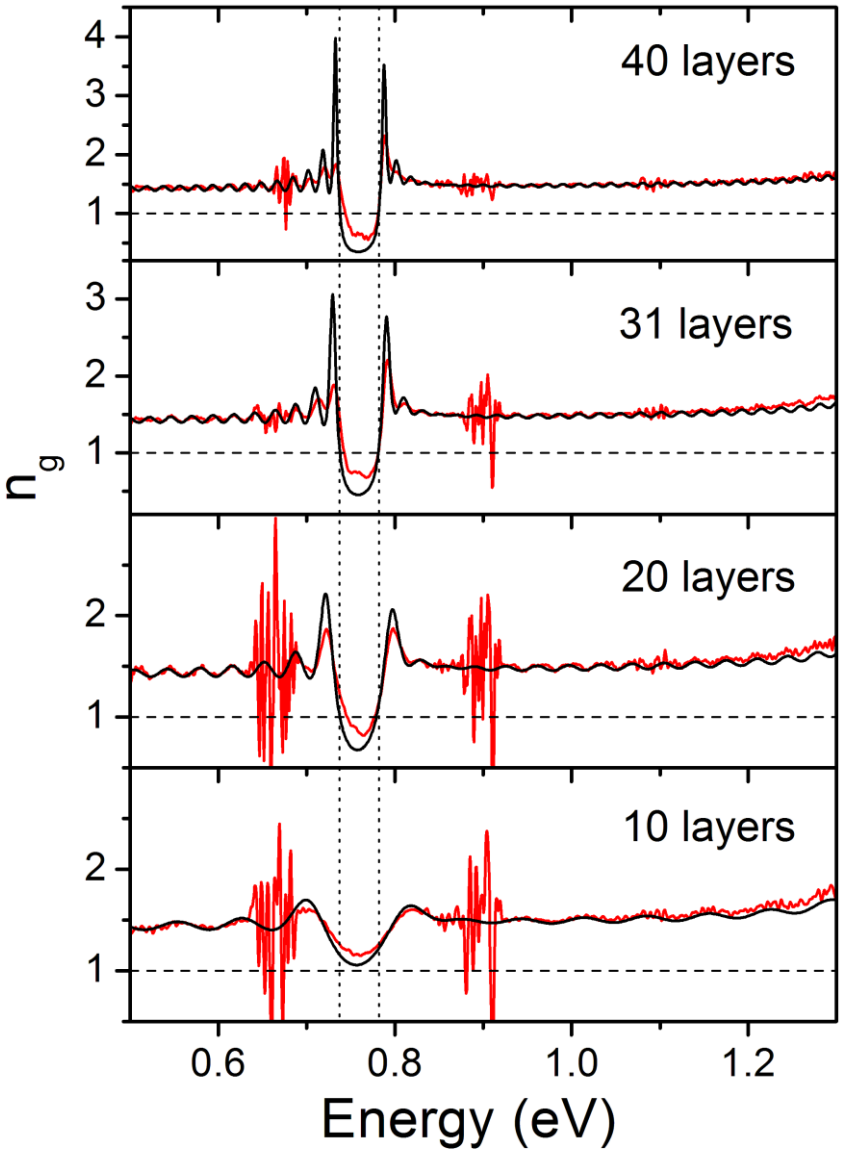

J.F. Galisteo-López *et al.* Figure 8

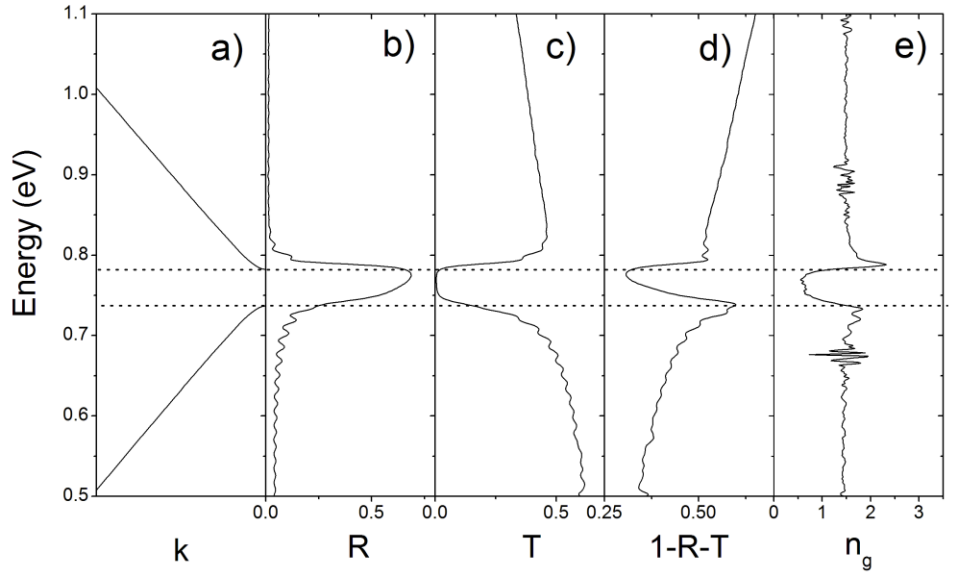

J.F. Galisteo-López *et al.* Figure 9

(Two column format)